A Lightweight Detector for Real-time Detection of Remote Sensing Images

Qianyi Wang Guoqiang Ren*

***Abstract*—Remote sensing imagery is widely used across various fields, yet real-time detection remains challenging due to the prevalence of small objects and the need to balance accuracy with efficiency. To address this, we propose DMG-YOLO, a lightweight real-time detector tailored for small object detection in remote sensing images. Specifically, we design a Dual-branch Feature Extraction (DFE) module in the backbone, which partitions feature maps into two parallel branches: one extracts local features via depthwise separable convolutions, and the other captures global context using a vision transformer with a gating mechanism. Additionally, a Multi-scale Feature Fusion (MFF) module with dilated convolutions enhances multi-scale integration while preserving fine details. In the neck, we introduce the Global and Local Aggregate Feature Pyramid Network (GLAFPN) to further boost small object detection through global-local feature fusion. Extensive experiments on the VisDrone2019 and NWPU VHR-10 datasets show that DMG-YOLO achieves competitive performance in terms of mAP, model size, and other key metrics.**

***Index Terms*— remote sensing ; small objects ; lightweight**

I. INTRODUCTION

REMOTE sensing images are utilized in various fields, including unmanned aerial vehicles (UAVs) [1], environmental monitoring [2], and disaster management [3]. The advancement of deep learning technology has significantly improved the performance of remote sensing image detection [4]. UAV-captured aerial images often contain small-scale, partially occluded objects due to low-altitude flight and complex environments. The wide field of view introduces significant background noise, increasing missed and false detections. These challenges, coupled with limited onboard resources and real-time processing demands, underscore the need for lightweight and efficient object detection algorithms.

Object detectors can be divided into two categories, one-stage and two-stage. Two-stage detectors such as R-CNN[5], Faster R-CNN [6], and Mask R-CNN [7]. Although these approaches attain high detection accuracy, their high computational complexity leads to slow inference times. In contrast, one-stage detectors, such as YOLO [8], offer superior real-time performance, albeit with a slight trade-off in accuracy compared to two-stage methods. YOLOv8 features a redesigned architecture with novel convolutional layers and an improved detection head, providing substantial enhancements in both speed and accuracy.

In recent years, many scholars have proposed their own improvement methods for the small object detection problem. Wang et al. [9] introduced the CSA module, which assembles spatial global features based on channel context information to increase the density of key information. Hou et al. [10] proposed C2f_GE, The module strengthens long-range dependency modeling by integrating pixel-level global context features. Wu et al. [11] constructed a new transformer decoder to extract contextual and channel information. Huang et al. [12] proposed the CST module, which improves the effectiveness of cross-layer feature transfer within the neck network.

Motivated by these improvements, this paper presents DMG-YOLO, aiming to detect small objects in remote sensing images in real time. The main contributions of this paper are as follows:

(1) We propose the Dual-branch Feature Extraction (DFE) module, which splits input feature channels into two parallel branches: one uses depthwise separable convolutions for local feature extraction, and the other integrates a vision transformer with a gating mechanism to capture global context. This dual-branch design enables multi-scale feature representation while controlling computational complexity.

(2) The SPPF module in YOLOv8 is replaced by ours proposed Multi-scale Feature Fusion (MFF) module. MFF adopts convolutional layers with different dilation rates to effectively aggregate multi-scale contextual information. Compared to the pooling operations in SPPF, this approach preserves finer spatial details.

(3) We propose a novel Global and Local Aggregate Feature Pyramid Network (GLAFPN), which incorporates specially designed global and local feature fusion modules to efficiently capture multi-scale information. By introducing cross-scale connections, GLAFPN facilitates effective integration of multi-scale features.

Qianyi Wang, Guoqiang Ren are with the Shandong University of science and technology, Jinan 250031, China (email: 202213040122@sdust.edu.cn;renguoqiang@sdust.edu.cn)

II.METHODOLOGY

The Network structure of DMG-YOLO is shown in Fig. 1 which follows the main architecture of YOLOv8. It can be divided into three parts: backbone, neck, and detection head.

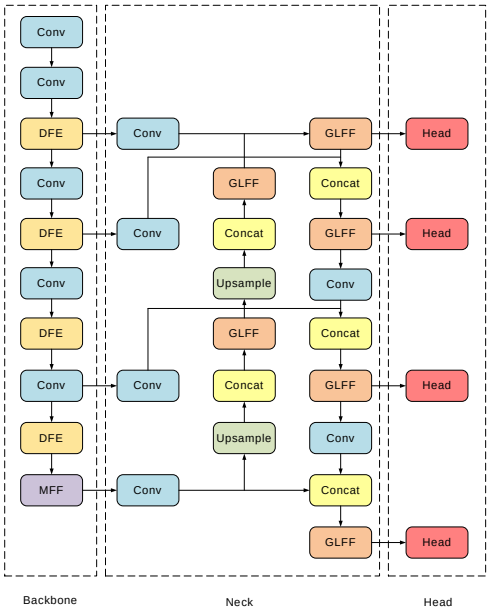

Fig. 1. Overall structure of DMG-YOLO.

A. Dual-branch Feature Extraction Module（DFE）

Conventional CNNs, constrained by fixed-size kernels, struggle to capture long-range dependencies. Vision Transformers (ViTs) [13] address this by modeling global context, improving feature representation under challenging conditions. However, their high computational cost hinders deployment in lightweight detectors like YOLO. To overcome this, we propose the DFE module, a hybrid extractor combining lightweight convolutions and a ViT. The structure of DFE module is shown in Fig. 2. The input is split into two branches: one processed by the CGLU-ViT for global context via self-attention, and the other by two depthwise separable convolutions (DWConv) with a residual connection to enhance local features.

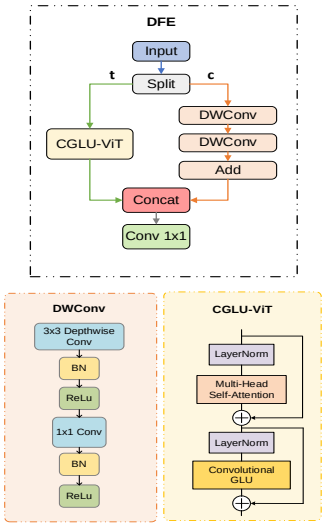

Fig. 2. Structure of DFE, DWConv and CGLU-ViT.

The outputs from both branches are fused via concatenation and refined through a convolutional layer to integrate and compress channel-wise information. This design synergizes the global context modeling of Transformers with the efficiency and locality of convolutions, enhancing feature expressiveness while maintaining computational efficiency.

The proposed CGLU-ViT module augments the standard Vision Transformer by incorporating convolutional gating for improved global-local feature representation. Input features undergo Layer Normalization and Multi-Head Self-Attention, followed by a residual connection to preserve gradient flow. The result is further normalized and processed by a Convolutional Gated Linear Unit (CGLU) [14], where a 3×3 depthwise separable convolution in the gated branch introduces local spatial awareness. A second residual connection maintains feature integrity. This hybrid architecture effectively integrates Transformer-based global modeling with convolutional local feature extraction. CGLU enhances local feature modeling and robustness by replacing coarse global pooling with deep convolution, effectively providing positional cues and improving perception of object boundaries and textures.

The structure of DFE module is shown in Fig. 3.

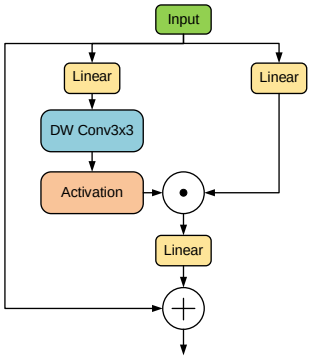

Fig. 3. Structure of CGLU.

B. Multi-scale Feature Fusion Module (MFF)

In YOLOv8, the SPPF achieves multi-scale feature fusion using a maximum pooling operation. Although pooling enhances computational efficiency, it compromises detailed feature representation. MFF utilizes convolutional layers with varying dilation rates to fuse features at different scales. The structure of MFF module is shown in Fig. 4.

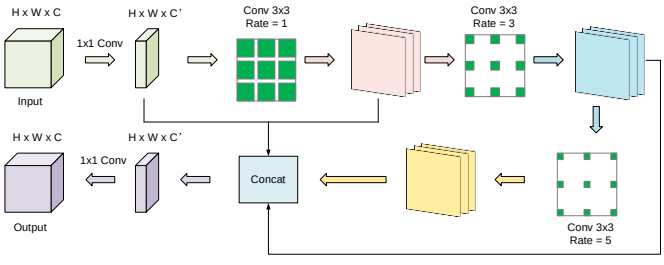

Fig. 4. Structure of MFF.

MFF employs a stacked structure of multiple dilated convolutions. Dilated convolution [15] inserts fixed gaps

between the elements of the convolution kernel to enlarge receptive field. For instance, when the dilation rate is k, each element of the kernel is spaced by $k-1$ gaps. The structure of dilated convolution is illustrated in Fig. 5.

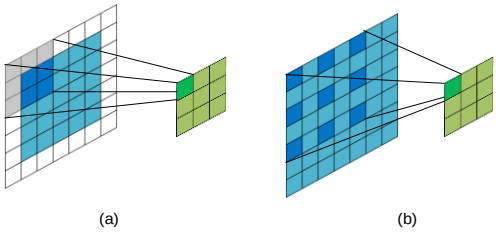

Fig. 5. Convolution (a) and dilated convolution (b).

The MFF operates as follows: the input image first undergoes channel adjustment through a 1×1 convolution. The resulting feature maps are then divided into two branches: one is directly connected to the final feature maps, while the other passes through three stacked dilated convolutional layers with rates of 1,3,5 respectively. Convolutional layers with small dilatation rates capture local information and convolutional layers with large dilatation rates capture global information. A residual connection is employed to integrate the feature maps with the final feature representation. Lastly, a 1×1 convolution is applied for cross-channel fusion. This architectural design enables effective multi-scale feature fusion by balancing local feature preservation and global context modeling.

C. Global and Local Aggregation Feature Pyramid Network (GLAFPN)

GLAFPN enhances cross-scale connectivity via bidirectional links between top-down and bottom-up pathways. However, shallow semantic features crucial for small object detection may be lost during fusion. To address this, we introduce an additional small-object layer within the top-down path to better preserve fine-grained details. This facilitates more effective multi-scale information flow and fusion. Additionally, the Global and Local Feature Fusion (GLFF) module is incorporated to balance global context and local details in multi-scale feature extraction. The architecture of GLSA is illustrated in Fig. 6.

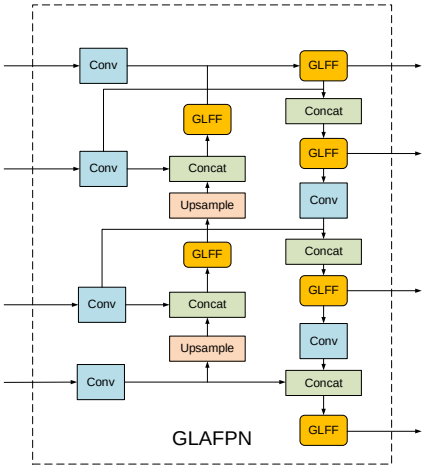

Fig. 6. Network structure of GLAFPN

Global attention facilitates the integration of contextual information, while local attention enables one to focus on detailed features. Inspired by the GLSA [16], we design the GLFF as the core module in GLAFPN to fuse global and local information. GLFF integrates GLSA to enhance the focus on global and local information. The structure of GLSA is shown in Fig. 7.

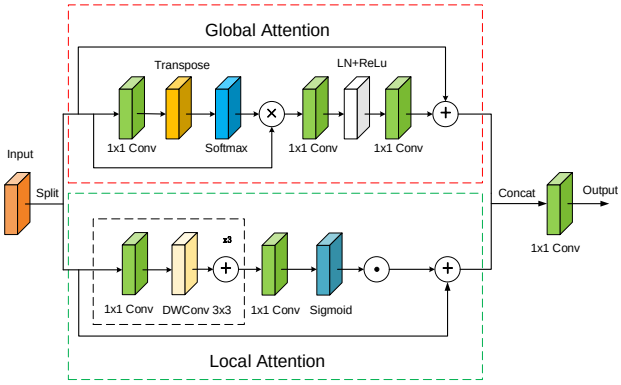

Fig. 7. Structure of GLSA module.

Specifically, the channel feature maps are evenly split into two groups and passed through the global spatial attention (GSA) module and local spatial attention (LSA) module, respectively. This process is formulated as follows:

$$\mathcal{F}_i^1, \mathcal{F}_i^2 = \mathrm{Split}(\mathcal{F}_i) \tag{1}$$

$$\mathcal{F}_i^{'} = \mathrm{C}_{1\times1}\left(\mathrm{Concat}\left(\mathrm{G}_{sa}(\mathcal{F}_i^1), \mathrm{L}_{sa}(\mathcal{F}_i^2)\right)\right) \tag{2}$$

where G_{sa} is the global spatial attention and L_{sa} is local space attention, $\mathcal{F}_i^{'}$ is the output features.

The GSA captures long-range dependencies between pixels in the images. By enabling remote interactions, its effectiveness is enhanced. The global spatial attention map is generated with $\mathcal{F}_i$ as input, formulated as follows:

$$\mathrm{Att}_G(\mathcal{F}_i^1) = Softmax\left(Transpose\left(\mathrm{C}_{1\times1}(\mathcal{F}_i^1)\right)\right) \tag{3}$$

$$\mathrm{G}_{sa}(\mathcal{F}_i^1) = MLP(\mathrm{Att}_G(\mathcal{F}_i^1) \otimes \mathcal{F}_i^1) + \mathcal{F}_i^1 \tag{4}$$

where $\mathrm{Att}_G(\cdot)$ represents the attention operation, $\mathrm{C}_{1\times1}$ denotes 1×1 convolution, and $\otimes$ signifies matrix multiplication. The module MLP$(\cdot)$ consists of two fully connected layers with a ReLU activation function and a normalization layer.

The LSA module efficiently captures local features, such as small objects. In brief, the local spatial attention response is computed with the local spatial attention response and as input as follows:

$$\mathrm{Att}_L(\mathcal{F}_i^2) = \sigma\left(\mathrm{C}_{1\times1}\left(\mathcal{F}_c(\mathcal{F}_i^2)\right) + \mathcal{F}_i^2\right) \tag{5}$$

$$\mathrm{L}_{sa} = \mathrm{Att}_L(\mathcal{F}_i^2) \odot \mathcal{F}_i^2 + \mathcal{F}_i^2 \tag{6}$$

where $\mathcal{F}_c(\cdot)$ denotes cascading three 1×1 convolution layers and 3×3 depth-wise convolution layers.

$Att_L(\cdot)$ is the local attention operation and $\sigma(\cdot)$ is the sigmoid function.

As shown in Fig. 8. The GLFF module first divides the input feature channels into two parts according to a predefined ratio. One part is retained as a shortcut connection, while the other is passed through a series of GLSA modules for further processing. The outputs from the GLSA modules are then concatenated with the shortcut features along the channel dimension, followed by a 1×1 convolution to fuse the features and adjust the channel dimensions. This design not only enhances the interaction between multi-scale features but also reduces redundant parameters, thereby improving both the efficiency and representational capacity of the network.

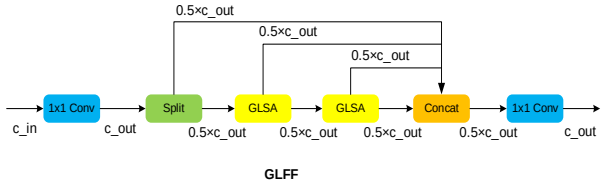

Fig. 8. Structure of GLFF module.

III.RESULTS

A. Datasets Introduction

VisDrone2019 dataset is an object detection dataset that contains images captured in everyday scenes by UAVs, with a focus on transportation (e.g., cars, trucks, buses) and pedestrians. NWPU VHR-10 dataset is a challenging geospatial object detection dataset comprising ten classes. In this paper, the division ratio of training set, testing set and validation set for both datasets is 8:1:1.

B. Training Setup

The experimental environment is configured as follows: Ubuntu 18.04, CUDA 12.0, PyTorch 2.0, 18 vCPUs on an AMD EPYC 9754 128-Core Processor, an RTX 4090 GPU, and 24 GB of RAM. The relevant parameters include 200 training epochs, at which point convergence is achieved. The input image size is set to 640x640, with a random seed of 1. Data augmentation is enabled, the optimizer used is SGD, and the learning rate is adjusted via gradient descent, with an initial value of 0.001.

C. Comparisons With Previous Methods

To evaluate DMG-YOLO, we conducted comparative experiments on the VisDrone2019 and NWPU VHR-10 datasets, using the lightweight n and s versions of the YOLO series to ensure real-time detection suitability. As shown in Tables I and Table II, on the VisDrone2019, DMG-YOLO improves mAP50 by 4.6%, reduces parameters by 0.5M, and adds only 3.8 GFLOPs compared to YOLOv11n. Compared with YOLOv11s, it slightly reduces mAP50 by 0.8% but significantly lowers both parameters and GFLOPs. On the NWPU VHR-10, DMG-YOLO outperforms YOLOv11n and YOLOv11s mAP50 by 8.6% and 0.7%, respectively. These results demonstrate that DMG-YOLO achieves an excellent balance between accuracy and efficiency.

TABLE I

COMPARISON OF DMG-YOLO AND OTHER MODELS ON VISDRONE2019.

Model	mAP50(%)	Params(M)	FLOPs(G)
YOLOv5n	32.5	1.8	4.2
YOLOv5s	36.7	9.1	24.1
YOLOv7-tiny	34.3	6.0	13.2
YOLOv8n	33.6	3.0	8.2
YOLOv8s	38.9	11.1	28.5
YOLOv10n	34.0	2.7	8.4
YOLOv10s	39.3	8.0	24.8
YOLOv11n	34.2	2.6	8.6
YOLOv11s	39.6	9.4	21.4
DMG-YOLO	38.8	2.1	12.4

TABLE II

COMPARISON OF DMG-YOLO AND OTHER MODELS ON NWPU VHR-10

Model	mAP50(%)	Params(M)	FLOPs(G)
YOLOv5n	82.1	1.8	4.2
YOLOv5s	88.3	9.1	24.1
YOLOv7-tiny	86.1	6.0	13.2
YOLOv8n	83.2	3.0	8.2
YOLOv8s	90.2	11.1	28.5
YOLOv10n	83.6	2.7	8.4
YOLOv10s	91.5	8.0	24.8
YOLOv11n	83.8	2.6	8.6
YOLOv11s	91.7	9.4	21.4
DMG-YOLO	92.4	2.1	12.4

D. Visualization

To evaluate the detection performance of DMG-YOLO and YOLOv8n on UAV imagery, two representative images were selected from VisDrone2019 and NWPU VHR-10, encompassing diverse scenes, lighting conditions, and viewing angles. Red circles highlight key detection areas to facilitate direct comparison. The detection results are presented in Fig. 9 and Fig. 10 respectively.

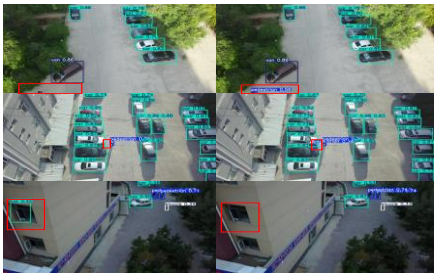

a b

Fig. 9. Detection results on VisDrone2019. (a) YOLOv8n (b) DMG-YOLO.

a b

Fig. 10. Detection results on NWPU VHR-10. (a) YOLOv8n (b) DMG-YOLO.

E. Ablation Experimental Result

To evaluate each module in DMG-YOLO, ablation experiments were conducted on VisDrone2019, with results shown in Table III. The baseline model achieved an mAP50 of 33.6%, with 3.01M parameters and 8.2 GFLOPs. Introducing the DFE module increased mAP50 to 34.4%, while parameters and GFLOPs decreased to 2.70M and 7.7, respectively, improving both accuracy and efficiency. Adding the MFF module further increased mAP50 to 35.0% without affecting parameter count, demonstrating effective feature fusion. With the GLAFPN module, mAP50 increased to 38.8%. Although GFLOPs rose from 7.8 to 12.4, parameters decreased to 2.15M, indicating improved accuracy alongside optimized model structure.

TABLE III

ABLATION EXPERIMENT RESULT IN VISDRONE2019.

DFE	MFF	GLAFPN	mAP50(%)	Params	FLOPs(G)
×	×	×	33.6	3012798	8.2
√	×	×	34.4	2699014	7.7
√	√	×	35.0	2760264	7.8
√	√	√	38.8	2146739	12.4

IV. CONCLUSION

This paper proposes DMG-YOLO, a lightweight real-time detector optimized for small object detection in UAV imagery. The proposed DFE module captures local and global context via a depthwise separable convolutional branch and a gated vision transformer branch. The MFF module employs dilated convolutions to retain fine-grained features, while the GLAFPN enhances multi-scale feature aggregation. Extensive experiments on VisDrone2019 and NWPU VHR-10 demonstrate that DMG-YOLO achieves competitive or superior performance in mAP, model size, and inference speed, validating its effectiveness for real-time remote sensing applications. Future work will focus on further optimization for edge deployment.

REFERENCES

[1] O. M. Bello, Y. A. J. P.-S. Aina, and B. Sciences, "Satellite remote sensing as a tool in disaster management and sustainable development: towards a synergistic approach," vol. 120, pp. 365-373, 2014.

[2] J. Li, Y. Pei, S. Zhao, R. Xiao, X. Sang, and C. J. R. S. Zhang, "A review of remote sensing for environmental monitoring in China," vol. 12, no. 7, p. 1130, 2020.

[3] O. M. Bello, Y. A. J. P.-S. Aina, and B. Sciences, "Satellite remote sensing as a tool in disaster management and sustainable development: towards a synergistic approach," vol. 120, pp. 365-373, 2014.

[4] L. Jiao et al., "A survey of deep learning-based object detection," vol. 7, pp. 128837-128868, 2019.

[5] R. Girshick, J. Donahue, T. Darrell, and J. Malik, "Rich feature hierarchies for accurate object detection and semantic segmentation," in Proceedings of the IEEE conference on computer vision and pattern recognition, 2014, pp. 580-587.

[6] R. Girshick, "Fast r-cnn," in Proceedings of the IEEE international conference on computer vision, 2015, pp. 1440-1448.

[7] K. He, G. Gkioxari, P. Dollár, and R. Girshick, "Mask r-cnn," in Proceedings of the IEEE international conference on computer vision, 2017, pp. 2961-2969.

[8] J. Redmon, S. Divvala, R. Girshick, and A. Farhadi, "You only look once: Unified, real-time object detection," in Proceedings of the IEEE conference on computer vision and pattern recognition, 2016, pp. 779-788.

[9] J. Wang et al., "Remote Sensing Small Object Detection Based on Multi-Contextual Information Aggregation," 2025.

[10] W. Hou et al., "Small Object Detection Method for UAV Remote Sensing Images Based on αS-YOLO," 2025.

[11] H. Wu, P. Huang, M. Zhang, W. Tang, X. J. I. T. o. G. Yu, and R. Sensing, "CMTFNet: CNN and multiscale transformer fusion network for remote-sensing image semantic segmentation," vol. 61, pp. 1-12, 2023.

[12] X. Huang, J. Zhu, Y. J. I. T. o. I. Huo, and Measurement, "SSA-YOLO: An improved YOLO for hot-rolled strip steel surface defect detection," 2024.

[13] A. Dosovitskiy et al., "An image is worth 16x16 words: Transformers for image recognition at scale," 2020.

[14] D. Shi, "Transnext: Robust foveal visual perception for vision transformers," in Proceedings of the IEEE/CVF conference on computer vision and pattern recognition, 2024, pp. 17773-17783.

[15]F. Yu, V. Koltun, and T. Funkhouser, "Dilated residual networks," in Proceedings of the IEEE conference on computer vision and pattern recognition, 2017, pp. 472-480.

[16] F. Tang et al., "DuAT: Dual-aggregation transformer network for medical image segmentation," in Chinese Conference on Pattern Recognition and Computer Vision (PRCV), 2023, pp. 343-356: Springer.